Maximum Likelihood Estimation of Power-Law Exponents for Testing Universality in Complex Systems

Víctor Navas-Portella, Álvaro González, Isabel Serra, Eduard Vives, and Álvaro Corral

Abstract Power-law-type distributions are extensively found when studying the behavior of many complex systems. However, due to limitations in data acquisition, empirical datasets often only cover a narrow range of observations, making it difficult to establish power-law behavior unambiguously. In this work, we present a statistical procedure to merge different datasets, with two different aims. First, we obtain a broader fitting range for the statistics of different experiments or observations of the same system. Second, we establish whether two or more different systems may belong to the same universality class. By means of maximum

V. Navas-Portella (✉)
Centre de Recerca Matemàtica, Bellaterra, Barcelona, Spain

Barcelona Graduate School of Mathematics, Barcelona, Spain

Facultat de Matemàtiques i Informàtica, Universitat de Barcelona, Barcelona, Spain
e-mail: vnavas@crm.cat

Á. González
Centre de Recerca Matemàtica, Bellaterra, Barcelona, Spain

GFZ German Research Centre for Geosciences, Potsdam, Germany

I. Serra
Centre de Recerca Matemàtica, Bellaterra, Barcelona, Spain

Barcelona Supercomputing Center, Barcelona, Spain

E. Vives
Departament de Matèria Condensada, Facultat de Física, Universitat de Barcelona, Barcelona, Catalonia, Spain

Universitat de Barcelona Institute of Complex Systems (UBICS), Facultat de Física, Universitat de Barcelona, Barcelona, Catalonia, Spain

Á. Corral
Barcelona Graduate School of Mathematics, Barcelona, Spain

Complexity Science Hub Vienna, Vienna, Austria

Departament de Matemàtiques, Universitat Autònoma de Barcelona, Barcelona, Spain

Centre de Recerca Matemàtica, Bellaterra, Barcelona, Spain

F. Font, T. G. Myers (eds.), *Multidisciplinary Mathematical Modelling*,
SEMA SIMAI Springer Series 11, https://doi.org/10.1007/978-3-030-64272-3_5

likelihood estimation, this methodology provides rigorous statistical information to discern whether power-law exponents characterizing different datasets can be considered equal to each other or not. This procedure is applied to the Gutenberg–Richter law for earthquakes and for synthetic earthquakes (acoustic emission events) generated in the laboratory: labquakes (Navas-Portella et al. Phys Rev E 100:062106, 2019).

1 Introduction

Generally speaking, a complex system can be understood as a large number of interacting elements whose global behavior cannot be derived from the local laws that characterize each of its components. The global response of the system can be observed at different scales, and the vast number of degrees of freedom hampers the prediction of the system dynamics. In this context, a probabilistic description of the phenomenon is needed in order to reasonably characterize it in terms of random variables. When the response of these systems exhibits lack of characteristic scales, it can be described in terms of power-law-type probability density functions (PDF), $f(x) \propto x^{-\gamma}$, where x corresponds to the values that can be taken by the random variable that characterizes the response the system can take, $\propto$ denotes the proportionality, and the power-law exponent γ acquires values larger than one. The power law is the only function that is invariant under any scale transformation of the variable x [1]. This property of scale invariance confers a description of the response of the system where there are no characteristic scales. This common framework is very usual in different disciplines [2, 3] such as condensed matter physics [4], economics [5], linguistics [6], geoscience [7], and, in particular, seismology [8, 9].

It has been broadly studied [10, 11] that different complex systems can be grouped into the same universality class when they present common values of all their power-law exponents and share the same scaling functions. Therefore, it is important to determine these exponents rigorously, not only to properly characterize phenomena but also to provide a good classification into universality classes.

In practice, exponents are difficult to measure empirically. Due to experimental limitations that distort the power-law behavior, the property of scale invariance can only be measured in a limited range. Therefore, when a power-law distribution is fitted to empirical data is more convenient to talk about local or restricted scale invariance. In this context, the wider the range the fitted PDF spans, the more reliable and strong this property will be.

A paradigmatic example of power-law behavior in complex systems is the well-known Gutenberg–Richter (GR) law for earthquakes [12]. This law states that, above a lower cut-off value, earthquake magnitudes follow an exponential distribution, in terms of the magnitude PDF,

$$f(m) = (b \log 10) 10^{-b(m-m_{min})} \propto 10^{-bm}, \tag{1}$$

defined for $m \geq m_{min}$, with m the magnitude (moment magnitude in our case), m_{min} the lower cut-off in magnitude, b is the so-called $b-$value, and log corresponds to the natural logarithm. The general relationship between seismic moment x and moment magnitude m is given by

$$x = 10^{\frac{3}{2}m+9.1}, \tag{2}$$

measured in units of Nm [13, 14]. Provided that in a change of variables such as $m \to x$ the probability is invariant, the following property must be true $f_X(x)dx = f_{\mathrm{m}}(m)dm$. Considering this probability invariance and combining Eqs. (1) and (2), the GR law is a power-law distribution when it is written as a function of the seismic moment x

$$f(x) = \frac{2}{3}\frac{b}{x_{min}}\left(\frac{x}{x_{min}}\right)^{-\left(1+\frac{2}{3}b\right)} = \frac{\gamma-1}{x_{min}}\left(\frac{x}{x_{min}}\right)^{-\gamma}, \tag{3}$$

where we conveniently define $\gamma = 1+\frac{2}{3}b$ ($b > 0$ and $\gamma > 1$), and x_{min} corresponds to the value of the seismic moment of the cut-off magnitude m_{min} [15] introduced in Eq. (2). Note that this PDF has a domain $x \in [x_{min}, +\infty)$.

An earthquake catalog is an empirical dataset that characterizes each earthquake by an array of observations: time of occurrence, spatial coordinates, magnitude, etc. The magnitude m_{min} is usually associated to the completeness threshold, such as all earthquakes with $m \geq m_{min}$ are recorded in the catalog [15]. For $m < m_{min}$, some events are missing from the catalog due to the difficulties of detecting them (e.g., [16, 17]), especially when the seismic activity rate suddenly increases, such as in aftershock sequences, in which earthquake waveforms tend to overlap each other and are difficult to detect [15, 18–20]. This incompleteness distorts the power-law behavior below m_{min}, whose value should be an upper bound to encompass these variations.

One has to keep in mind that there also exists an upper cut-off due to finite-size effects [21], implying that, at a certain value of the magnitude, there are deviations from the power-law behavior. Consequently, strictly speaking, the range of validity of the GR law cannot be extended up to infinity [7, 22]. By ignoring which is the model that conveniently fits the tail of the distribution, the power-law behavior has to be restricted to an upper cut-off x_{max}. By considering a generic power-law distribution $f_X(x) = Cx^{-\gamma}$, where C is a normalizing constant and the support $x \in [x_{min}, x_{max}]$, the PDF for the truncated GR law is written as

$$f(x) = \frac{1-\gamma}{x_{max}^{1-\gamma} - x_{min}^{1-\gamma}}x^{-\gamma}, \tag{4}$$

defined for $x \in [x_{min}, x_{max}]$.

Recent studies regarding the acoustic emission (AE) in compression experiments of porous glasses and minerals [23–28] or wood [29] have focused the attention

on the energy distribution of AE events due to the similarities with the GR law for earthquakes [22]. According to the terminology that is used in some of these studies, we will name as labquakes those AE events that occur during the compression of materials.

Earthquake and labquake catalogs as well as other empirical datasets in complex systems only report a limited range of events, making it difficult to estimate parameters of the power-law PDF accurately. In this work, we try to solve this problem by combining datasets with rigorous statistical tools, with the goal of finding a broader range of validity when the different datasets correspond to the same system. If different datasets can be combined and characterized by a unique power-law exponent, it means that the particular exponents of each dataset are statistically compatible. When different phenomena share the same power-law exponents for the distributions of all their observables, they can be classified into the same universality class. Consequently, this methodology represents a statistical technique to discern whether different phenomena can be classified into the same universality class or not.

In order to conveniently classify earthquakes and labquakes into the same universality class, all the observables should be taken into account and all the corresponding exponents should be compatible. In this work, we will illustrate this methodology by focusing on the distribution of seismic moment for earthquakes and the AE energy for labquakes. The results will reveal whether they are candidates to be classified into the same universality class or not, but the final establishment of their belonging to the same universality class would require the study of all the possible observables.

The manuscript is structured as follows: Sect. 2 deals with the procedure of mergin datasets. This method is first tested with synthetic data (Sect. 3). The earthquake and charcoal labquake catalogs used are presented in Sect. 4, which also explores the effect of the data resolution in the fitting procedure. Earthquake catalogs are merged in Sect. 5 and then merged with labquake catalogs in Sect. 6. The conclusions are set out in Sect. 7.

2 Merging Datasets

By considering n_{ds} datasets of N_i ($i = 1, \ldots, n_{\mathrm{ds}}$) observations each, one wants to fit a general power-law distribution with a unique global exponent for all of them. Let us assume that for the i-th dataset, the variable X (seismic moment if one works with the GR law for earthquakes or AE energy if one works with the GR law for labquakes) follows a power-law PDF $f_X(x; \gamma_i, x_{min}^{(i)}, x_{max}^{(i)})$ given by Eq. (4) from a certain lower cut-off $x_{min}^{(i)}$ to an upper cut-off $x_{max}^{(i)}$ with exponent γ_i and number of data n_i ($n_i \leq N_i$) in the range $\left[x_{min}^{(i)}, x_{max}^{(i)}\right]$. Note that one can also consider the untruncated power-law model for the i-th dataset if $x_{max}^{(i)} \to \infty$. One can state that

data from the i-th dataset does not lead to the rejection of the power-law hypothesis for a certain range (see Refs. [7, 30], or alternatively, Ref. [31]). Note that, in the i-th dataset, the variable $\mathcal{X}$ can acquire values in a range typically spanning several orders of magnitude.

Generally, the procedure of merging datasets is performed by selecting upper and lower cut-offs $x_{min}^{(i)}$ and $x_{max}^{(i)}$ ($x_{min}^{(i)} < x_{max}^{(i)}$) for each dataset. Note that "merging" does not imply that events as a whole are grouped together but their values of the corresponding observable under study are instead lumped together to a new dataset. Data outside these ranges are not considered. All the possible combinations of cut-offs $\{x_{min}\}$ and $\{x_{max}\}$ are checked with a fixed resolution (see below). The Residual Coefficient of Variation (CV) test can be used to fix some upper cut-offs, thus reducing the computational effort. For more details about the CV test applied in this context, see Ref. [32]. Two models can be tested:

- **Model One Exponent (OneExp)**: All datasets are merged by considering a unique global exponent Γ ($\gamma_i = \Gamma$ for all datasets).
- **Model Multi Exponent (MultiExp)**: All datasets are merged, but each one with its own exponent γ_i ($i = 1, \ldots, n_{\text{ds}}$).

Note that model OneExp is nested in model MultiExp and the difference in the number of parameters characterizing these models is $n_{\mathcal{L}}^{(MultiExp)} - n_{\mathcal{L}}^{(OneExp)} = n_{ds} - 1$. Since one is interested in merging datasets with a unique global exponent (model OneExp), enough statistical evidence that this simpler model is suitable to fit the data is needed. The fit is performed by means of the following protocol:

0. **Select a given set of cut-offs** $\left[x_{min}^{(i)}, x_{max}^{(i)}\right]$, $(x_{min}^{(i)} < x_{max}^{(i)})$ for $i = 1, \ldots, n_{ds}$.
1. **Maximum likelihood estimation (MLE) of model OneExp**: The log-likelihood function of model OneExp can be written as

$$\log \mathcal{L}_{OneExp} = \sum_{i=1}^{n_{\text{ds}}} \sum_{j=1}^{n_i} \log f_{\mathcal{X}}\left(x_{ij}; \Gamma, x_{min}^{(i)}, x_{max}^{(i)}\right), \tag{5}$$

where x_{ij} corresponds to the n_i values of the variable $\mathcal{X}$ that are in the range $x_{min}^{(i)} \leq x_{ij} \leq x_{max}^{(i)}$ in the i-th dataset, log is the natural logarithm, and Γ is the global exponent. The definition of likelihood is consistent with the fact that likelihoods from different datasets can be combined in this way [33, p. 27]. At this step, one has to find the value $\hat{\Gamma}$ of the global exponent Γ that maximizes the log-likelihood expression in Eq. (5). For the particular expressions corresponding to the untruncated and truncated power-law PDF, see Eqs. (3) and (4). If all the power-law distributions are untruncated, this exponent can be easily found analytically [34] as

$$\hat{\Gamma} = 1 + \frac{\sum_{i=1}^{n_{ds}} n_i}{\sum_{i=1}^{n_{ds}} \frac{n_i}{\hat{\gamma}_i - 1}},$$

where the hats denote the values of the exponents that maximize the log-likelihood of the particular power-law distribution (model MultiExp) and the general one in Eq. (5). See Ref. [34] for more details about the relationship between the global and particular exponents. If truncated power-law distributions are considered, one has to use a numerical method in order to determine the exponent $\hat{\Gamma}$ that maximizes this expression [30, 35].

2. **MLE of model MultiExp**: The log-likelihood function of the model MultiExp can be written as

$$\log \mathcal{L}_{MultiExp} = \sum_{i=1}^{n_{\rm ds}} \sum_{j=1}^{n_i} \log f_{\mathcal{X}} \left(x_{ij}; \gamma_i, x_{min}^{(i)}, x_{max}^{(i)} \right) , \tag{6}$$

using the same notation as in Eq. (5). For the particular expressions corresponding to the truncated and untruncated power-law PDFs, see Eqs. (4) and (3) in Sect. 2. The values of the exponents that maximize Eq. (6) are denoted as $\hat{\gamma}_i$.

3. **Likelihood ratio test**: The likelihood ratio test (LRT) for the models OneExp and MultiExp is used to check whether the model OneExp is good enough to fit the data or not in comparison with the model MultiExp. For more details about the LRT applied in this context, see Ref. [32]. If the model OneExp is not rejected, the procedure goes to step (4). Otherwise, this fit is discarded and the procedure goes back to step (0). Note that the model OneExp can be a good model to fit if the particular exponents $\hat{\gamma}_i$ do not exhibit large differences among each other in relation to their uncertainty.
4. **Goodness-of-fit test**: In order to check whether it is reasonable to consider the model OneExp as a good candidate to fit the data, the next null hypothesis is formulated H_0: the variable $\mathcal{X}$ is power-law distributed with the global exponent $\hat{\Gamma}$ for all the datasets. Two different statistics used in order to carry out the goodness-of-fit tests are used: the Kolmogorov–Smirnov Distance of the Merged Datasets (KSDMD) and the Composite Kolmogorov–Smirnov Distance (CKSD). The KSDMD statistic can be used as long as datasets overlap each other, whereas the CKSD statistic does not require this condition. For more details about how these statistics are defined and how the p-value of the test is found, see Ref. [32]. If the resulting p-value is greater than a threshold value p_c (in the present work, the thresholds $p_c = 0.05$ and $p_c = 0.20$ are used), this is considered as a valid fit and it can be stated that the variable $\mathcal{X}$ is power law distributed with exponent $\hat{\Gamma}$ along all the different datasets for the different ranges $\{x_{min}\}$ and $\{x_{max}\}$. Otherwise, this fit is not be considered as valid and the procedure goes back to step (0).

When all the combinations of cut-offs have been checked, one may have a list of valid fits. In order to determine which of them is considered the definitive, the following procedure is carried out:

1. The fit that covers the largest sum of orders of magnitude $\max\left[\sum_{i=1}^{n_{ds}} \log_{10}\left(\frac{x_{max}^{(i)}}{x_{min}^{(i)}}\right)\right]$ is chosen. If the power-law fit is untruncated, $x_{max}^{(i)}$ can be substituted by the maximum observed value $x_{top}^{(i)}$. If there is a unique candidate with a maximum number of orders of magnitude, then this is considered as the definitive global fit. Otherwise, the procedure goes to the next step.
2. The fit with the broadest global range $\max\left[\frac{\max\left(x_{max}^{(i)}\right)}{\min\left(x_{min}^{(i)}\right)}\right]$ for $i = 1, \ldots, n_{ds}$ is chosen. If there is a unique candidate, this is considered as the definitive global fit. Otherwise, the procedure goes to the next step.
3. The fit with the maximum number of data $\mathcal{N} = \sum_{i=1}^{n_{ds}} n_i$ is considered as the definitive global fit.

By means of these three steps, a unique fit has been found for all the datasets analyzed in this work. Nevertheless, one could deal with datasets in which more conditions are needed in order to choose a definitive fit unambiguously. In this case, the protocol formally concludes either by considering a subset of valid fits or choosing one of them according to the researcher's criteria. At the end of this procedure, if a unique solution is found, one is able to state that the datasets that conform the global fit correspond to phenomena that are candidates to be classified into the same universality class, at least regarding the observable $\mathcal{X}$. If no combination of cut-offs is found to give a good fit, then it can be said that there exists at least one catalog that corresponds to a phenomenon that must be classified in a different universality class.

3 Performance Over Synthetic Datasets

Once the methodology for merging datasets has been presented together with the different goodness-of-fit tests, it is important to check the performance of the method over synthetic data. In order to carry out this analysis, two untruncated power-law-distributed datasets with exponents γ_1 and γ_2, lower cut-offs $x_{min}^{(1)}$ and $x_{min}^{(2)}$, and sizes n_1 and n_2 are generated. In order to simplify the analysis, the sizes of both datasets are considered to be equal, $n_1 = n_2$. The global exponent $\hat{\Gamma}$ of the merged catalogs is estimated according to the methodology explained in the main text, and the LRT statistic $2\mathcal{R}_e$ is computed according to the methods presented in Sect. 2. Given that the difference on parameters between model 1 and 2 in this case is 1, the critical value of the test with a level of risk equal to 0.05 is $2\mathcal{R}_c = 3.84$. If the empirical LRT statistic is found to be larger than the critical one, one then rejects the null hypothesis that the simpler model 1 is good enough to describe data and, consequently, more parameters are needed. Once the global exponent and the likelihood ratio statistic are found, the two different goodness-of-fit tests explained in Ref. [32] are performed.

The analysis is performed for different dataset sizes as well as different power-law exponents γ_1 and γ_2. The results of the method for synthetic datasets are shown in Table 1. Five groups are presented depending on the relative difference δ_γ between exponents. The p-values of the CKSD and KSDMD goodness-of-fit tests have been computed with 10^4 Monte Carlo simulations. In order to compare our results with a test that checks whether two power-law exponents are significantly different or not, the p_{norm}-value of the z-test detailed in Ref. [9] is also shown. These p-values can be computed by assuming that, for a sufficiently large sample size, the z-statistic follows a normal distribution with zero mean and standard deviation equal to one. As one would expect, if both datasets have exactly the same power-law exponent, the null hypothesis that variable X is power-law-distributed for all the datasets with the global exponent $\hat{\Gamma}$ is not rejected. When the CKSD goodness-of-fit test rejects the null hypothesis of a power-law distribution with a global exponent, the z-test also rejects the null hypothesis of considering $\gamma_1 = \gamma_2$. The same does not apply for the KSDMD goodness-of-fit test, where some fits yield to non-rejectable p-values, whereas the z-test clearly rejects the null hypothesis. In this sense, one can consider that the KSDMD statistic is less strict than the CKSD statistic. However, for the sample sizes that are involved in this work, both goodness-of-fit tests reject the null hypothesis for sufficiently large difference in the exponents. It can also be seen that the null hypothesis is rejected independently on the goodness-of-fit test for those fits in which the Likelihood Ratio statistic exceeds the critical value $2\mathcal{R}_c = 3.84$. This fact justifies the decision of performing the LRT before the goodness-of-fit test.

4 Earthquake and Charcoal Labquake Catalogs

We have selected catalogs that have different completeness magnitudes in order to cover different magnitude ranges. We hope that a convenient combination of these datasets will give us a larger range of validity of the GR law with a unique exponent. Let us briefly describe the catalogs that have been used in this work (see also Fig. 1):

- Global Centroid Moment Tensor (CMT) Catalog: It comprises earthquakes worldwide since 1977 [36, 37], from which we analyze the dataset until the end of 2017. This catalog reports the values of the moment magnitude as well as the seismic moment. Given that the seismic moment is provided with three significant digits, the resolution of the magnitude in the catalog is approximately $\Delta m \simeq 10^{-3}$.
- Yang–Hauksson–Shearer (YHS) A: It records earthquakes in Southern California with $m \geq 0$ in the period 1981–2010 [38]. This catalog does not report the seismic moment but a preferred magnitude that is approximately converted into seismic moment according to Eq. (2). The resolution of the catalog is $\Delta m = 0.01$.

Table 1 Performance of the methodology for merging datasets explained in the main text for two untruncated power laws with exponents γ_1 and γ_2, lower cut-offs $x_{min}^{(1)} = 10^{12}$ and $x_{min}^{(2)} = 10^{14}$ (arbitrary units), and sizes n_1 and n_2. σ_1 and σ_2 correspond to the standard deviations of the MLEs. Five different groups are presented depending on the relative difference of the power-law exponents δ_γ. For these datasets, the fitted global exponent $\hat{\Gamma}$ is estimated and the LRT statistic $2\mathcal{R}_e$ is computed. The statistics $D_e^{(CKSD)}$ and $D_e^{(KSDMD)}$ together with their corresponding p-values p_{value}^{CKSD} and p_{value}^{KSDMD} are presented for each combination of datasets. As a complement, the z-statistic and the p-value p_{norm}-z from to the z-test are also shown

n_1	γ_1	σ_1	n_2	γ_2	σ_2	δ_γ (%)	$\hat{\Gamma}$	$2\mathcal{R}_e$	$D_e^{(CKSD)}$	p_{value}^{CKSD}	$D_e^{(KSDMD)}$	p_{value}^{KSDMD}	z	p_{norm}-z
10^2	1.50	0.05	10^2	1.50	0.05	0	1.471	0.624	1.635	0.425	0.075	0.453	0.788	0.431
10^3	1.50	0.02	10^3	1.50	0.02	0	1.503	1.284	1.316	0.801	0.023	0.595	1.132	0.257
10^4	1.50	0.005	10^4	1.50	0.005	0	1.501	0.139	1.289	0.837	0.009	0.986	0.373	0.707
10^2	1.53	0.05	10^2	1.50	0.05	2	1.484	1.443	1.660	0.395	0.070	0.578	1.195	0.232
10^3	1.53	0.02	10^3	1.50	0.02	2	1.518	0.029	1.239	0.876	0.017	0.893	0.170	0.865
10^4	1.53	0.005	10^4	1.50	0.005	2	1.516	14.037	3.187	5×10^{-4}	0.013	0.024	3.745	1.81×10^{-4}
10^2	1.575	0.058	10^2	1.50	0.05	5	1.514	3.154	1.815	0.249	0.058	0.755	1.755	0.079
10^3	1.575	0.018	10^3	1.50	0.02	5	1.541	2.458	2.032	0.111	0.031	0.180	1.567	0.117
10^4	1.575	0.006	10^4	1.50	0.005	5	1.536	64.957	4.740	0	0.029	0	9.474	0
10^2	1.65	0.065	10^2	1.50	0.05	10	1.528	6.956	2.262	0.046	0.054	0.832	2.571	0.010
10^3	1.65	0.02	10^3	1.50	0.02	10	1.57	22.365	3.369	10^{-4}	0.044	0.015	4.690	2.73×10^{-6}
10^4	1.650	0.007	10^4	1.50	0.005	10	1.566	329.552	10.601	0	0.053	0	17.933	0
10^2	1.725	0.073	10^2	1.50	0.05	15	1.551	11.566	2.661	0.008	0.090	0.260	3.262	0.001
10^3	1.725	0.023	10^3	1.50	0.02	15	1.598	51.266	4.608	0	0.066	10^{-4}	7.026	2.12×10^{-12}
10^4	1.725	0.007	10^4	1.50	0.005	15	1.593	667.096	14.507	0	0.075	0	25.204	0

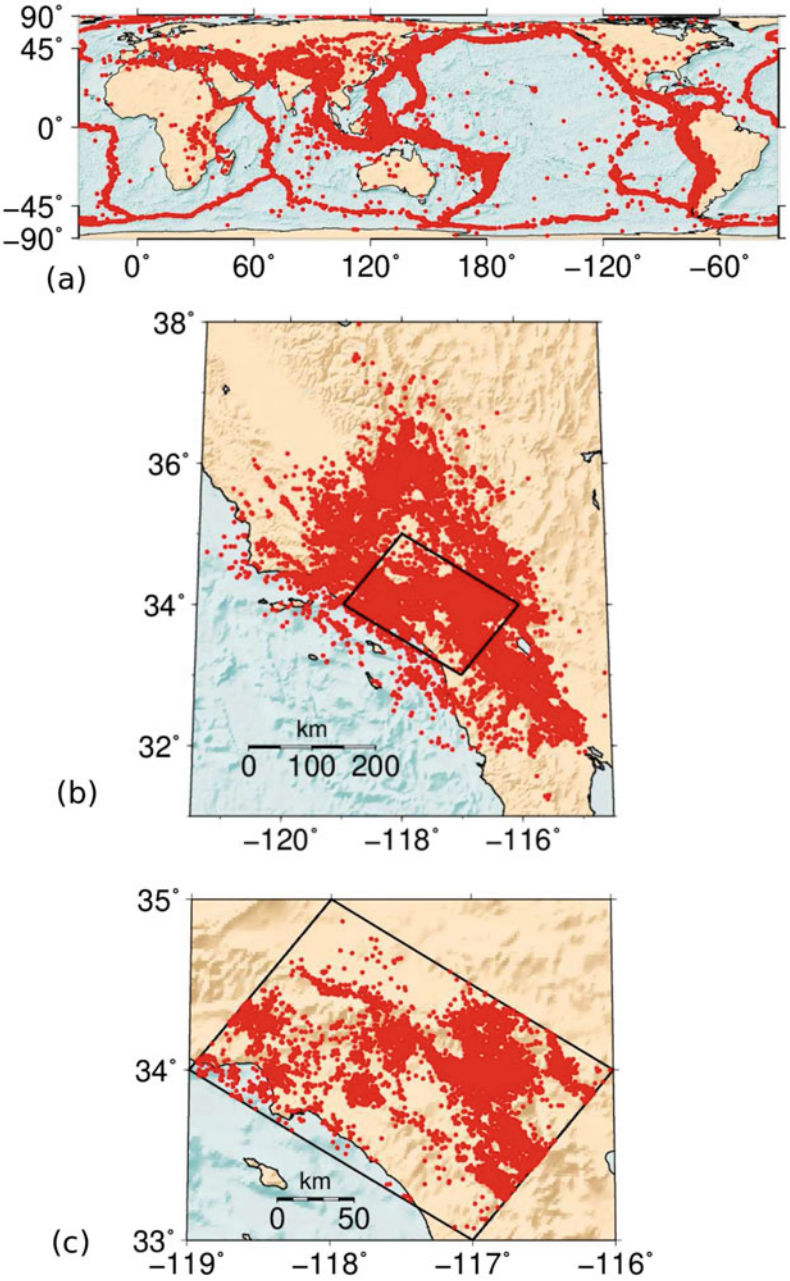

Fig. 1 Earthquake epicenters of the different catalogs. Horizontal and vertical axes correspond to longitude and latitude in degrees, respectively. (**a**) Full CMT catalog for the period 1977–2017 [36, 37]. (**b**) Entire YHS A Catalog [38] of Southern California for the period 1981–2010. (**c**) Subcatalog corresponding to a region (YHS B) of the YHS catalog for Los Angeles area for the period 2000–2010. Maps in cylindrical equal-area projection (top) and sinusoidal projection (middle and bottom), produced with Generic Mapping Tools [39]

- Yang–Hauksson–Shearer (YHS) B: It is a subset of YHS A that contains the earthquakes in the region of Los Angeles in the period 2000–2010 [38]. This LA region is defined by the following four vertices in longitude and latitude: $(119°W, 34°N)$,$(118°W, 35°N)$,$(116°W, 34°N)$, and $(117°W, 33°N)$ (see Fig. 1). This region has been selected because it is among the best monitorized ones [17, 40]. Furthermore, we selected this time period due to the better detection of small earthquakes than in previous years [40], which should reduce the completeness magnitude of the catalog [17]. The magnitude resolution of this catalog is the same as YHS A.

Figure 1 shows the epicentral locations of the earthquakes contained in each catalog. In the statistical analysis, in order to not to count the same earthquake more than once, the spatio-temporal window corresponding to the YHS B catalog has been excluded from the YHS A and the spatio-temporal window corresponding to the YSH A catalog has been excluded from the CMT catalog.

We performed one uniaxial compression experiment of charcoal in a conventional test machine Z005 (Zwick/Roell). Samples with no lateral confinement were placed between two plates that approached each other at a certain constant displacement rate $\dot{z}$. Simultaneous to the compression, recording of an AE signal was performed by using a piezoelectric transducer embedded in one of the compression plates. The electric signal $U(t)$ was pre-amplified, band filtered (between 20 kHz and 2 MHz), and analyzed by means of a PCI-2 acquisition system from Euro Physical Acoustics (Mistras Group) with an AD card working at 40 megasamples per second with 18 bits precision [41]. Signal pre-amplification was necessary to record small AE events. Some values of the pre-amplified signal were so large that could not be detected correctly by the acquisition system. This fact led to signal saturation and, consequently, an underestimated energy of the AE event [34]. Recording of data stopped when a big failure event occurred, and the sample got destroyed.

An AE event (often called AE hit in specialized AE literature) starts at the time t_j when the signal $U(t)$ exceeds a fixed detection threshold and finishes at time $t_j + \tau_j$ when the signal remains below threshold from $t_j + \tau_j$ to at least $t_j + \tau_j + 200\,\mu s$. The energy E_j of each event is determined as $E_j = \frac{1}{R}\int_{t_j}^{t_j+\tau_j} U^2(t)dt$, where R is a reference resistance of $10\,k\Omega$. This AE energy corresponds to the radiated energy received by the transducer. At the end of an experiment, a catalog of events is collected, each of them characterized by a time of occurrence t_j, energy E_j, and duration τ_j.

4.1 Effect of the Magnitude Resolution in Earthquake Catalogs

A different issue that can be addressed is whether the magnitude resolution in earthquake catalogs affects the fitting procedures when PDFs are considered as continuous. As explained in Sect. 4, some catalogs provide the magnitudes with

a given resolution Δm, leading to discretized values when they are transformed into seismic moments in order to fit a power-law distribution. In order to check the effect of the resolution Δm when fitting a power law, n exponentially distributed magnitudes were generated according to the Gutenberg–Richter law (assuming $b = 1$ and $m_{min} = 3$) from uniform random numbers u according to

$$m = m_{min} - \frac{\log_{10}(1-u)}{b}.$$

Once generated, these values were binned according to the bin width or resolution Δm and converted into seismic moment according to Eq. (2). The fitting procedure explained in Sect. 2 was then applied, and the results for different sample sizes ($n = 10^2$, $n = 10^3$ and $n = 10^4$) of magnitudes sampled from a Gutenberg–Richter law (b-value$= 1$ and $m_{min} = 3$) and discretized according to different values of the resolution Δm are shown in Table 2.

In Fig. 2, the fitted $\hat{b}$-value as a function of the resolution Δm is shown for the three different sample sizes. As it can be observed, the value of the maximum

Table 2 Results of simulating magnitudes sampled from a Gutenberg–Richter law with $m_{min} = 3$ and b-value$= 1$ for different sample sizes n and different resolutions Δm. The fitted $\hat{b}$-values and their standard deviations σ were computed by means of MLE, and p-values were extracted from the KS goodness-of-fit test explained in Ref. [30]. Data are plotted in Fig. 2

Δm	m_{min}	b-value	n	$\hat{b}$	σ	p_{value}
1	3	1	10^2	3.948	0.394	0
			10^3	4.4326	0.140	0
			10^4	4.024	0.040	0
0.5	3	1	10^2	1.448	0.145	0
			10^3	1.876	0.059	0
			10^4	1.840	0.018	0
0.1	3	1	10^2	1.070	0.106	0
			10^3	1.113	0.035	0
			10^3	1.122	0.011	0
0.05	3	1	10^2	0.994	0.099	0.022 ± 0.001
			10^3	1.060	0.033	0
			10^4	1.086	0.011	0
0.01	3	1	10^2	1.050	0.105	0.578 ± 0.004
			10^3	1.013	0.032	0.267 ± 0.004
			10^4	0.997	0.010	0
0.005	3	1	10^2	1.076	0.108	0.856 ± 0.004
			10^3	1.039	0.033	0.396 ± 0.005
			10^4	0.995	0.010	0.033 ± 0.002
0.001	3	1	10^2	1.067	0.102	0.588 ± 0.005
			10^3	1.018	0.0322	0.828 ± 0.004
			10^4	1.009	0.010	0.386 ± 0.005

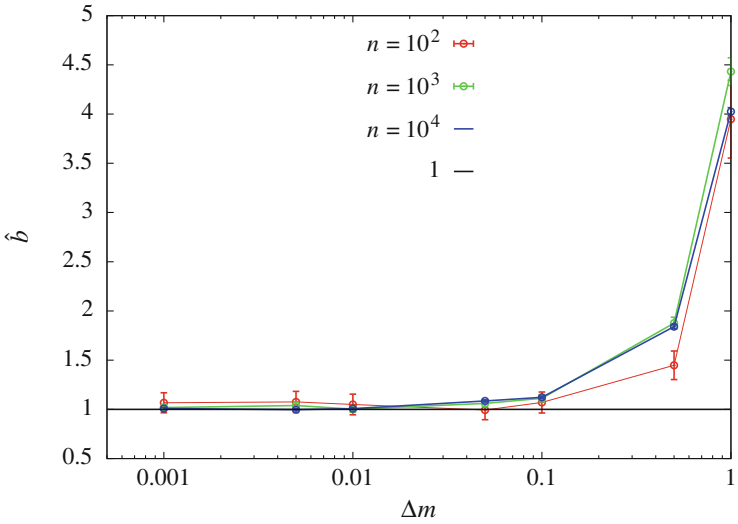

Fig. 2 Maximum likelihood estimator $\hat{b}$-value as a function of the resolution in magnitudes Δm for different sample sizes. Data are sampled from a Gutenberg–Richter law with $m_{min} = 3$ and b-value$= 1$. The horizontal black line corresponds to the real b-value. Data are shown in Table 2

likelihood (ML) estimator converges to the expected b-value$= 1$ as the magnitude bin width is decreased. The ML estimator is biased for resolutions larger than 0.1 and is acceptable, within the error bars, for smaller values of the resolution [42]. However, the results of the goodness-of-fit test lead to rejectable p-values for large samples even when the ML estimator is unbiased (see Table 2). A resolution of $\Delta m = 10^{-3}$ ensures that the largest sample of $n = 10^4$ yields non-rejectable p-values. Some results presented in this chapter deal with catalogs whose resolution and number of events could result in rejectable fits. However, non-rejectable p-values were found instead, leading to the conclusion that data in those real catalogs follow a power-law distribution even more reliably.

5 Merging Earthquake Catalogs

The GR law states that the seismic moment can be considered as a random variable $\mathcal{M}$ that is power-law distributed. In its usual form, the GR law fits a power-law model that contemplates a unique power-law exponent. Nevertheless, several studies have elucidated the existence of a double-power-law behavior in the GR law for global seismicity [7, 43, 44]. Corral and Gonzalez [7] pointed out that a truncated power law with exponent $\gamma \simeq 1.66$ cannot be rejected up to $m_{max} \simeq 7.4$ and a second power-law tail emerges from $m'_{min} = 7.67$ with an exponent $\gamma'_M = 2.1 \pm 0.1$. Furthermore, by fixing the upper truncation at $m_{max} = m'_{min} = 7.67$, the truncated

power-law hypothesis cannot be rejected (see Table 3). Consequently, if one wishes to fit a power-law PDF with a unique exponent, all those earthquakes with $m \geq m_{max} = 7.67$ should be excluded. For the CMT catalog, the upper cut-off is fixed at $M_{max} = 10^{\frac{3}{2}m_{max}+9.1}$, whereas the other catalogs can be safely fitted by untruncated power-law PDFs because the CV test does not reject the hypothesis of a unique power-law tail and the magnitudes that are studied are considerably smaller than those in the CMT catalog (see Table 3).

Therefore, two untruncated power-law distributions and a third one that is truncated for the CMT catalog are considered in order to merge catalogs. For each decade, 5 values of $M_{min}^{(i)}$ equally spaced in logarithmic scale are sampled, and all the possible combinations of cut-offs $M_{min}^{(1)}$, $M_{min}^{(2)}$, and $M_{min}^{(3)}$ are checked for a fixed upper truncation $M_{max}^{(3)}$. The labels (1), (2), and (3) correspond to the catalogs YSH B, YSH A, and CMT, respectively.

In Table 4, the results of the global fit for models OneExp and MultiExp are shown. The same global fit is found independently from the choice of the test statistic used in the goodness-of-fit test. A b-value very close to one holds for more than 8 orders of magnitude in seismic moment from $m_{min} = 1.93$ to $m_{max} = 7.67$ (see Fig.3). The value of the global exponent is approximately in agreement with the harmonic mean of the particular exponents of the GR law for each catalog [34, 45]. Due to the upper truncation, the value of the global exponent is not exactly the same as the value of the harmonic mean of the particular exponents. The results for the CKSD statistic do not show remarkable differences if the critical p-value is set to $p_c = 0.20$ (see Table 4). The definitive fit is the one whose goodness-of-fit test has been performed with a threshold value of $p_c = 0.20$.

This is the broadest fitting range that has been found for the Gutenberg–Richter law for earthquakes with a unique value of the exponent [9]. There are catalogs of tiny mining-induced earthquakes that exhibit a much smaller completeness magnitude [46] than the ones of natural seismicity used in this work. They were not considered here because they are not currently public and show b-values significantly different [47] from the one found here, which would result in non-acceptable fits when merging them with the other catalogs, possibly pointing to a different universality class.

6 Merging Earthquake and Labquake Catalogs: Universality

Motivated by the fact that the power-law exponents of earthquake catalogs and charcoal labquakes are very similar, the methodology for merging datasets explained in Sect. 2 is here applied by adding also the catalog of charcoal labquakes.

Table 3 Results of fitting the GR law for each individual catalog. The total number of earthquakes in each catalog is given by N, whereas the number of data entering into the fit is n. The value m_{top} corresponds to the maximum observed value for each catalog. The GR law is valid for each catalog from $[m_{min}, m_{max}]$ with a particular b-value. m_{max} has no upper limit for any of the fits except for the CMT catalog, in which $m_{max}^{(3)} = 7.67$ (so $M_{max}^{(3)} = 4.03 \times 10^{20}$ Nm). Numbers in parentheses correspond to the error bars estimated with one σ in the scale given by the last digit. The p-value of the fits has been computed with 10^3 simulations and $p_c = 0.05$

	N	n	m_{min}	M_{min} (Nm)	m_{top}	M_{top}(Nm)	$\hat{b}$-value	$\hat{\gamma}_M$	p_{fit}
(1) YHS B	26330	3412	1.93	10^{12}	5.39	1.53×10^{17}	0.99(3)	1.66(2)	0.072(8)
(2) YHS A	152924	4353	3.17	7.08×10^{13}	7.20	7.94×10^{19}	0.98(1)	1.65(1)	0.080(9)
(3) CMT	48637	22336	5.33	1.24×10^{17}	9.08	5.25×10^{22}	0.982(7)	1.655(5)	0.36(2)

Table 4 Results of fitting the models OneExp and MultiExp to the earthquake catalogs when performing the goodness-of-fit test with the CKSD statistics and different values of p_c. If the goodness-of-fit test is performed with the KSDMD statistic, the same set of cut-offs as the fit done by using $\text{CKSD}_{0.20}$ is found. Same symbols as in Table 3. OM corresponds to the orders of magnitude, and $\hat{b}_g$-value is the global b-value$= \frac{3}{2}(\Gamma_M - 1)$. The value $M_{max}^{(i)}$ is replaced for $M_{top}^{(i)}$ for untruncated fits. Note that $7.67 - 1.93 = 5.74$ units in magnitude correspond to 8.6 orders of magnitude in seismic moment

Model MultiExp	n	M_{min}	M_{min} (Nm)	OM	$\hat{b}$-value	$\hat{\gamma}_M$	p_{fit}
(1) YHS B	3412	1.93	10^{12}	5.18	0.99(1)	1.633(7)	0.072(8)
(2) YHS A	3500	3.27	10^{14}	5.90	0.99(2)	1.66(1)	0.089(9)
(3) CMT	19,003	5.40	1.58×10^{17}	3.40	0.98(8)	1.655(5)	0.26(1)
Model OneExp	$\mathcal{N}$			$\sum$OM	$\hat{b}_g$-value	$\hat{\Gamma}_M$	p_{fit}
$p_c = 0.05$	25,915	1.93	10^{12}	14.48	0.991(6)	1.661(4)	0.079(9)
Model MultiExp	n	M_{min}	M_{min} (Nm)	OM	$\hat{b}$-value	$\hat{\gamma}_M$	p_{fit}
(1) YHS B	3412	1.93	10^{12}	5.18	0.99(1)	1.633(7)	0.072(8)
(2) YHS A	3500	3.27	10^{14}	5.90	0.99(2)	1.66(1)	0.089(9)
(3) CMT	10,422	5.67	3.98×10^{17}	3	1.00(1)	1.663(7)	0.62(2)
Model OneExp	$\mathcal{N}$			$\sum$OM	$\hat{b}_g$-value	$\hat{\Gamma}_M$	p_{fit}
$p_c = 0.20$	17,334	1.93	10^{12}	14.08	1.000(8)	1.667(5)	0.326(5)

It is important to stress the fact that the seismic moment does not correspond with the radiated energy E_r by the earthquake, which would be the reasonable energy to compare with the AE energy. For this study, the ratio of seismically radiated energy over the seismic moment is considered as constant so that the values of the seismic moment should just be multiplied by a unique factor. The value of this unique factor is $\frac{E_r}{M} = 10^{-4.6}$ [14], where M is the seismic moment. In this case, E_r corresponds to the energy radiated in seismic waves by earthquakes and the AE energy.

It can be shown that, for both models OneExp and MultiExp, multiplying the variable by a constant factor only introduces a constant term in the log-likelihood that does not change neither its maximum nor the difference of the log-likelihoods. Let us suppose n_{ds} datasets and that data in the i-th dataset is described, for simplicity and without losing generality, in terms of untruncated power-law PDFs. The log-likelihood function for both OneExp and MultiExp models are, respectively,

$$\begin{aligned} \log \mathcal{L}_{OneExp} &= \sum_{i=1}^{n_{ds}} \sum_{j=1}^{n_i} \log f_{\mathcal{X}}\left(x_{ij}\right) \\ &= \sum_{i=1}^{n_{ds}} \sum_{j=1}^{n_i} \log \left(\frac{\Gamma - 1}{x_{min}^{(i)1-\Gamma}} x_{ij}^{-\Gamma} \right) . \end{aligned} \tag{7}$$

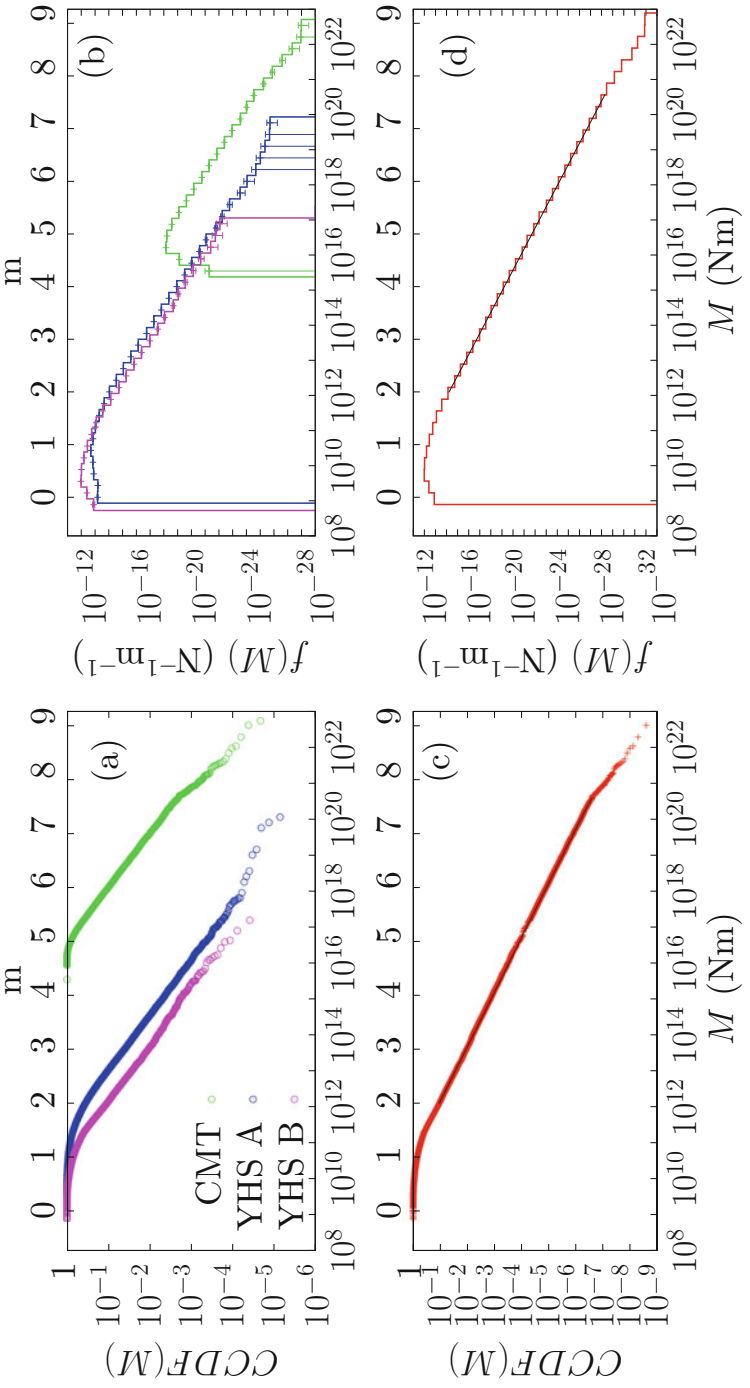

Fig. 3 Estimated Complementary Cumulative Distribution Functions (CCDF) of the Gutenberg–Richter law for each earthquake catalog (**a**) and for the merged catalogs (**c**). Estimated PDFs $f(M)$ of the Gutenberg–Richter law for each catalog (**b**) and for the merged catalogs (**d**). The merged histogram is plotted by following the procedure explained in Ref. [34]. Fits are represented by solid black lines. Top axis represents the same scale in moment magnitude

$$\begin{aligned}\log \mathcal{L}_{MultiExp} &= \sum_{i=1}^{n_{ds}} \sum_{j=1}^{n_i} \log f_{\mathcal{X}}\left(x_{ij}\right) \\ &= \sum_{i=1}^{n_{ds}} \sum_{j=1}^{n_i} \log \left(\frac{\gamma_i - 1}{x_{min}^{(i)1-\gamma_i}} x_{ij}^{-\gamma_i} \right) .\end{aligned} \tag{8}$$

Let us now suppose that the values taken by the variable $\mathcal{X}$ in the i-th dataset are multiplied by a certain factor λ_i as well as the lower cut-off $x_{min}^{(i)}$

$$x_{ij} \rightarrow \lambda_i x_{ij} ,$$

$$x_{min}^{(i)} \rightarrow \lambda_i x_{min}^{(i)} .$$

Note that this is not strictly speaking a scale transformation since not only the variable but some parameters characterizing the function are changed. The likelihoods of the transformed data $\mathcal{L}^T$ for both models are

$$\begin{aligned}\log \mathcal{L}_{OneExp}^T &= \sum_{i=1}^{n_{ds}} \sum_{j=1}^{n_i} \log \left(\frac{\Gamma - 1}{\left(\lambda_i x_{min}^{(i)}\right)^{1-\Gamma}} \left(\lambda_i x_{ij}\right)^{-\Gamma} \right) \\ &= \log \mathcal{L}_{OneExp} - \sum_{i=1}^{n_{ds}} n_i \log \lambda_i ,\end{aligned} \tag{9}$$

$$\begin{aligned}\log \mathcal{L}_{MultiExp}^T &= \sum_{i=1}^{n_{ds}} \sum_{j=1}^{n_i} \log \left(\frac{\gamma_i - 1}{\left(\lambda_i x_{min}^{(i)}\right)^{1-\gamma_i}} \left(\lambda_i x_{ij}\right)^{-\gamma_i} \right) \\ &= \log \mathcal{L}_{MultiExp} - \sum_{i=1}^{n_{ds}} n_i \log \lambda_i .\end{aligned} \tag{10}$$

The transformed likelihoods can be expressed in terms of the likelihood functions of the original data together with an additive constant term that does not depend neither on the exponent nor the cut-off. This means that the maximum of the transformed log-likelihood is attained at exactly the same value as the maximum of the original one. Given that the likelihood ratio statistic is a subtraction of the likelihood of both models, the relation between the original statistic $2\mathcal{R}$ and the one

corresponding to transformed likelihood functions is

$$\begin{aligned} 2\mathcal{R}^T &= 2\left(\log \mathcal{L}^T_{MultiExp} - \log \mathcal{L}^T_{OneExp}\right) \\ &= 2\left(\log \mathcal{L}_{MultiExp} - \log \mathcal{L}_{OneExp}\right) = 2\mathcal{R}\,. \end{aligned} \tag{11}$$

Since the two additional terms in the transformed likelihoods are the same for both models, they cancel and the statistic for the likelihood ratio test is invariant under this transformation. As the CKSD statistic is a weighted average of the particular KS distances of each dataset, it does not change either. Therefore, the results shown in Table 3 would not change except for the values of the cut-offs.

The CV test does not reject the hypothesis of a unique power-law tail for the charcoal labquake catalog, and an untruncated power-law model is considered for this catalog [32]. Therefore, three untruncated power laws are fitted for the charcoal and YSH B and YSH A catalogs, and a truncated power law is fitted to the CMT catalog. For each decade, 5 different values of $x^{(i)}_{min}$ equally spaced in logarithmic scale, for a fixed upper truncation $x^{(3)}_{max}$, were checked, and all the possible combinations of cut-offs $x^{(0)}_{min}$, $x^{(1)}_{min}$, $x^{(2)}_{min}$, and $x^{(3)}_{min}$ are checked for a fixed upper truncation $x^{(3)}_{max}$. The labels (0), (1), (2), and (3) correspond to the catalogs of the charcoal experiment, YSH B, YSH A, and CMT, respectively.

The results of the global fit for the CKSD statistic are presented in Table 5. In this case, not all the catalogs overlap each other and the CKSD statistic is the only one that can be used for the goodness-of-fit test. The value of the global exponent is approximately in agreement with the harmonic mean of the particular exponents of

Table 5 Results of fitting models OneExp and MultiExp to the charcoal labquake and earthquake datasets for two different values of p_c. Same notation as in previous tables. Note that E_r represents the radiated energy in seismic waves by earthquakes and the radiated AE energy (Nm = Joule)

Model MultiExp	n	m_{min}	$E_{r,min}$ (Nm)	OM	$\hat{b}$-value	$\hat{\gamma}_{E_r}$	p_{fit}
(0) Charcoal	15,906	–	6.31×10^{-18}	6.47	0.988(8)	1.658(5)	0.15(1)
(1) YHS B	1353	2.33	9.99×10^{7}	4.58	0.98(3)	1.66(2)	0.10(1)
(2) YHS A	234	4.47	1.59×10^{11}	4.10	0.98(6)	1.65(4)	0.62(2)
(3) CMT	7689	5.80	1.59×10^{13}	2.80	1.00(1)	1.667(9)	0.393(5)
Model OneExp	$\mathcal{N}$			$\sum$OM	$\hat{b}_g$-value	$\hat{\Gamma}_{E_r}$	p_{fit}
$p_c = 0.05$	25182		6.3×10^{-18}	17.95	1.003(6)	1.669(4)	0.057(7)
Model MultiExp	n	m_{min}	$E_{r,min}$ (Nm)	OM	$\hat{b}$-value	$\hat{\gamma}_{E_r}$	p_{fit}
(0) Charcoal	3555	–	6.31×10^{-17}	5.47	1.04(2)	1.69(1)	0.88(1)
(1) YHS B	1007	2.47	1.59×10^{8}	4.38	0.99(3)	1.66(2)	0.058(7)
(2) YHS A	234	4.47	1.59×10^{11}	4.10	0.98(6)	1.65(4)	0.62(2)
(3) CMT	3014	6.20	6.33×10^{13}	2.20	1.00(2)	1.67(2)	0.59(2)
Model OneExp	$\mathcal{N}$			$\sum$OM	$\hat{b}_g$-value	$\hat{\Gamma}_{E_r}$	p_{fit}
$p_c = 0.20$	7810		6.3×10^{-17}	16.15	1.03(1)	1.688(8)	0.21(1)

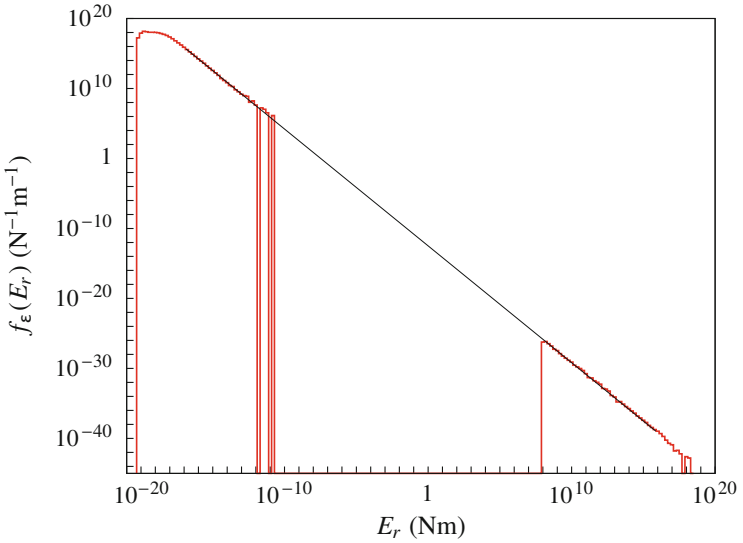

Fig. 4 Estimated PDF of the radiated energy E_r for the merged earthquake and charcoal labquake catalogs. The fit is represented by a solid black line. The methodology to construct the histogram with the three earthquake catalogs is the same as the one explained in Ref. [34], whereas the addition of the labquake histogram to this fit has been done ad hoc by conveniently rescaling both parts (those corresponding to labquakes and earthquakes, respectively). Each part has been divided by an effective number of events by assuming that the probability in each part corresponds to that obtained from a global power-law exponent with exponent $\hat{\Gamma}$ from $x_{min}^{(0)}$ to $x_{max}^{(3)}$. Note that events from the CMT, YSH A, and YSH B catalogs below their respective lower cut-offs x_{min} have been excluded in the plot

the GR law for each catalog [34]. The results do not show remarkable differences if the critical p-value is set to $p_c = 0.20$ (see Table 5). The definitive fit is the one whose goodness-of-fit test has been performed with a threshold value of $p_c = 0.20$. These results are shown in Fig. 4 and are compatible with the ones obtained from synthetic catalogs shown in Sect. 3.

Given that there is no overlapping between the charcoal labquake catalog and the earthquake ones, an alternative procedure must be applied in order to construct the histogram of the estimated global PDF. First, the three earthquake catalogs are merged according to the procedure detailed in Sect. 2. The earthquakes from the CMT catalog that are above the upper cut-off $x_{max}^{(4)}$ are also plotted, but they are not part of the global PDF. Earthquakes from the YSH B, YSH A, and CMT catalogs that are below $x_{min}^{(2)}$, $x_{min}^{(3)}$ and $x_{min}^{(4)}$, respectively, are also excluded. This piece of the histogram, which is not normalized yet, is denoted as Ea, from earthquakes. The charcoal labquake catalog histogram is plotted without normalizing by any number of events yet. The piece of histogram corresponding to charcoal labquakes is denoted as La, from labquakes. Given that no normalization has been performed yet, at this point of the procedure, the pieces (Ea) and (La) are not aligned in logarithmic

scale. Consequently, the fit of a global power law with exponent $\hat{\Gamma}$ from $x_{min}^{(1)}$ to $x_{max}^{(4)}$ will not overlap with both pieces.

In order to align both pieces, one has to assume that data from $x_{min}^{(1)}$ to $x_{max}^{(4)}$ follows a power-law distribution with exponent $\hat{\Gamma}$. Given that this assumption is supported by statistical results that have been already found, it can be imposed that the probability represented by each piece corresponds to this theoretical probability. In order to achieve this imposition, the total number of counts in each piece is divided by the effective number of events in that piece

$$F\left(x = x_{top}^{(1)}; x_{min}^{(1)}, x_{max}^{(4)}, \hat{\Gamma}\right) - F\left(x = x_{min}^{(1)}; x_{min}^{(1)}, x_{max}^{(4)}, \hat{\Gamma}\right) = \frac{C\left(x_{min}^{(1)} \leq x \leq x_{top}^{(1)}\right)}{n_{eff}^{La}},$$

$$F\left(x = x_{max}^{(4)}; x_{min}^{(1)}, x_{max}^{(4)}, \hat{\Gamma}\right) - F\left(x = x_{min}^{(2)}; x_{min}^{(1)}, x_{max}^{(4)}, \hat{\Gamma}\right) = \frac{C\left(x_{min}^{(2)} \leq x \leq x_{max}^{(4)}\right)}{n_{eff}^{Ea}},$$

where $C()$ corresponds to the number of counts in the interval considered inside the parenthesis, F corresponds to the CDF of a truncated power law

$$F\left(x = x_{min}^{(1)}; x_{min}^{(1)}, x_{max}^{(4)}, \hat{\Gamma}\right) = 0\,.$$

Note that these numbers are integers for the (La) piece, but not for the (Ea) given that it has been constructed by merging several datasets and an event does not contribute necessarily one unit (see Ref. [34]). By dividing the piece (Ea) by n_{eff}^{Ea} and the piece (La) by n_{eff}^{La}, the histograms are aligned and overlapping with the theoretical fit. However, given that data outside the fit is also considered in the construction of the histogram, the integral of both pieces (Ea) and (La) will not be one and the effective area A_{eff} at this point corresponds to

$$A_{eff} = \frac{C\left(x_{low}^{(1)} \leq x \leq x_{top}^{(1)}\right)}{n_{eff}^{La}} + \frac{C\left(x_{min}^{(2)} \leq x \leq x_{top}^{(4)}\right)}{n_{eff}^{Ea}}\,.$$

In order to normalize the PDF, both pieces together with the theoretical fit must be divided by A_{eff}. Contrarily to the procedure to construct a merged histogram explained in Ref. [34], this procedure is performed ad hoc in the sense that the theoretical PDF needs to be known a priori in order to obtain a graphical representation.

Earthquake catalogs have also been merged with a charcoal labquake catalog with a global power-law exponent $\hat{\Gamma}_{E_r} = 1.688$, suggesting that these different systems would be classified into the same universality class. Further investigations involving different observables, such as the distribution of waiting times, might be

necessary in order to properly classify charcoal labquakes and real earthquakes into the same universality class.

7 Conclusions

We have presented a statistical procedure to merge different datasets in order to validate the existence of universal power-law exponents across different scales or phenomena. This methodology can be useful in the study of different complex systems in order to check whether the power-law exponents obtained via maximum likelihood estimation are statistically compatible among them. Therefore, the procedure presented in this paper provides a statistical tool that enables to establish whether different complex systems can be classified into the same universality class. This work extends the results presented in [32], exploring the effect on the fits of the magnitude resolution in earthquake catalogs, and detailing the mathematical derivations.

In this work, the methodology has been applied to the Gutenberg–Richter law for earthquakes and labquakes. By merging earthquake catalogs, a global power law with a global exponent $\Gamma = 1.667$ holds for more than 8 orders of magnitude in seismic moment (from $m_{min} = 1.93$ to $m_{max} = 7.67$ in moment magnitude). To our knowledge, this is the broadest fitting range that has been found for the Gutenberg–Richter law for earthquakes with a unique value of the exponent [48]. There are catalogs of tiny mining-induced earthquakes that exhibit a much smaller completeness magnitude [46] than the ones of natural seismicity used in this work. They were not considered here because they are not currently public and show b-values significantly different [47] from the one found here, which would result in non-acceptable fits when merging them with the rest of catalogs, possibly pointing to a different universality class. Future works involving different earthquake catalogs can be carried out in order to find a broader fitting range of the Gutenberg–Richter laws and also to check whether different regions have compatible power-law exponents or not. This kind of studies would be of interest in order to statistically strengthen the geological arguments that justify the difference in the b-values observed in some regions [45].

Earthquake catalogs have also been merged with a charcoal labquake catalog with a global power-law exponent $\Gamma = 1.688$ suggesting that these different systems might be classified into the same universality class. Further investigations involving different observables, such as the distribution of waiting times, would be necessary in order to properly classify charcoal labquakes and real earthquakes into the same universality class.

Acknowledgments The research leading to these results has received funding from "La Caixa" Foundation. V. N. acknowledges financial support from the Spanish Ministry of Economy and Competitiveness (MINECO, Spain), through the "María de Maeztu" Programme for Units of Excellence in R & D (grant no. MDM-2014-0445) and the Juan de la Cierva research contract

FJCI-2016-29307 hold by Á.G.. We also acknowledge financial support from the MINECO under grant nos. FIS2015-71851-P, FIS-PGC2018-099629-B-100, and MAT2016-75823-R and from the Agència de Gestió d'Ajuts Universitaris i de Recerca (AGAUR) under grant no. 2014SGR-1307.

References

1. Christensen, K., Moloney, N.R.: Complexity and Criticality. Imperial College Press London (2005)
2. Bak, P.: How Nature Works: The Science of Self-organized Criticality. Oxford University Press, Oxford (1997)
3. Sethna, J.P., Dahmen, K.A., Myers, C.R.: Crackling noise. Nature **410**(6825), 242–250 (2001)
4. Salje, E.K.H., Dahmen, K.A.: Crackling noise in disordered materials. Annu. Rev. Cond. Matter Phys. **5**(1), 233–254 (2014)
5. Gabaix, X.: Power laws in economics: An introduction. J. Econ. Pers. **30**(1), 185–206 (2016)
6. Moreno-Sánchez, I., Font-Clos, F., Corral, A.: Large-scale analysis of Zipf's law in English texts. PLOS One **11**(1), 1–19 (2016)
7. Corral, Á., González, Á.: Power-law distributions in geoscience revisited. Earth Space Sci. **6**, 673–697 (2019)
8. Kagan, Y.Y.: Earthquakes: Models, Statistics, Testable Forecasts. Wiley, London (2013)
9. Kagan, Y.Y.: Earthquake size distribution: power-law with exponent $\beta \equiv \frac{1}{2}$? Tectonophysics **490**(1), 103–114 (2010)
10. Stanley, H.E.: Scaling, universality, and renormalization: three pillars of modern critical phenomena. Rev. Mod. Phys. **71**, S358–S366 (1999)
11. Stanley, H.E., Amaral, L.A.N., Gopikrishnan, P., Ivanov, P.Ch., Keitt, T.H., Plerou, V.: Scale invariance and universality: organizing principles in complex systems. Phys. A Stat. Mech. App. **281**(1), 60–68 (2000)
12. Utsu, T.: Representation and analysis of the earthquake size distribution: a historical review and some new approaches. Pure Appl. Geophys. **155**(2–4), 509–535 (1999)
13. Hanks, T.C., Kanamori, H.: A moment magnitude scale. J. Geophys. Res. Solid Earth **84**(B5), 2348–2350 (1979)
14. Bormann, P.: Are new data suggesting a revision of the current M_w and M_e scaling formulas? J. Seismol. **19**(4), 989–1002 (2015)
15. Woessner, J., Wiemer, S.: Assessing the quality of earthquake catalogues: estimating the magnitude of completeness and its uncertainty. Bull. Seismol. Soc. Am. **95**(2), 684–694 (2005)
16. González, Á.: The Spanish national earthquake catalogue: evolution, precision and completeness. J. Seism. **21**(3), 435–471 (2017)
17. Schorlemmer, D., Woessner, J.: Probability of detecting an earthquake. Bull. Seismol. Soc. Am. **98**(2), 2103–2117 (2008)
18. Davidsen, J., Green, A.: Are earthquake magnitudes clustered? Phys. Rev. Lett. **106**, 108502 (2011)
19. Hainzl, S.: Rate-dependent incompleteness of earthquake catalogs. Seism. Res. Lett. **87**(2A), 337–344 (2016)
20. Helmstetter, A., Kagan, Y.Y., Jackson, D.D.: Comparison of short-term and time-independent earthquake forecast models for Southern California. Bull. Seismol. Soc. Am. **96**(1), 90–106, 02 (2006)
21. Corral, Á., García-Millán, R., Moloney, N.R., Font-Clos, F.: Phase transition, scaling of moments, and order-parameter distributions in Brownian particles and branching processes with finite-size effects. Phys. Rev. E **97**, 062156 (2018)
22. Serra, I., Corral, Á.: Deviation from power law of the global seismic moment distribution. Sci. Rep. **7**(1), 40045 (2017)

23. Baró, J., Corral, Á., Illa, X., Planes, A., Salje, E.K.H. Schranz, W., Soto-Parra, D.E., Vives, E.: Statistical similarity between the compression of a porous material and earthquakes. Phys. Rev. Lett. **110**(8), 088702 (2013)
24. Nataf, G.F., Castillo-Villa, P.O., Baró, J., Illa, X., Vives, E., Planes, A., Salje, E.K.H.: Avalanches in compressed porous SiO_2-based materials. Phys. Rev. E **90**(2), 022405 (2014)
25. Navas-Portella, V., Corral, Á., Vives , E.: Avalanches and force drops in displacement-driven compression of porous glasses. Phys. Rev. E **94**(3), 033005 (2016)
26. Yoshimitsu, N., Kawakata, H., Takahashi, N.: Magnitude −7 level earthquakes: a new lower limit of self-similarity in seismic scaling relationships. Geophys. Res. Lett. **41**(13), 4495–4502 (2014)
27. Main, I.G.: Little earthquakes in the lab. Physics **6**:20 (2013)
28. Uhl, J.T., Pathak, S., Schorlemmer, D., Liu, X., Swindeman, R., Brinkman, B.A.W., LeBlanc, M., Tsekenis, G., Friedman, N., Behringer, R., Denisov, D., Schall, P., Gu, X., Wright, W.J., Hufnagel, T., Jennings, A., Greer, J.R., Liaw, P.K., Becker, T., Dresen, G., Dahmen, K.A.: Universal quake statistics: from compressed nanocrystals to earthquakes. Sci. Rep. **5**, 16493 (2015)
29. Mäkinen, T., Miksic, A., Ovaska, M., Alava, M.J.: Avalanches in wood compression. Phys. Rev. Lett. **115**(5), 055501 (2015)
30. Deluca, A., Corral, Á.: Fitting and goodness-of-fit test of non-truncated and truncated power-law distributions. Acta Geophys. **61**(6), 1351–1394 (2013)
31. Clauset, A., Shalizi, C.R., Newman, M.E.J.: Power-law distributions in empirical data. SIAM Rev. **51**, 661–703 (2009)
32. Navas-Portella, V., Serra, I., González, Á., Vives, E., Corral, Á.: Universality of power-law exponents by means of maximum likelihood estimation. Phys. Rev. E **100**, 062106 (2019)
33. Pawitan, Y.: In All Likelihood: Statistical Modelling and Inference Using Likelihood. OUP Oxford, Oxford (2013)
34. Navas-Portella, V., Serra, I., Corral, Á., Vives, E.: Increasing power-law range in avalanche amplitude and energy distributions. Phys. Rev. E **97**, 022134 (2018)
35. Baró, J., Vives, E.: Analysis of power-law exponents by maximum-likelihood maps. Phys. Rev. E **85**(6), 066121 (2012)
36. Chou, T.-A., Dziewonski, A.M., Woodhouse, J.H.: Determination of earthquake source parameters from waveform data for studies of global and regional seismicity. J. Geophys. Res **86**, 2825–2852 (1981)
37. Nettles, M., Ekström, G., Dziewonski, A.M.: The Global CMT project 2004–2010: centroid-moment tensors for 13,017 earthquakes. Phys. Earth Planet. Inter. **200–201**, 1–9 (2012)
38. Yang, W., Hauksson, E., Shearer, P.M.: Computing a large refined catalog of focal mechanisms for Southern California (1981–2010): temporal stability of the style of faulting. Bull. Seismol. Soc. Am. **102**, 1179–1194 (2012)
39. Wessel, P., Luis, J., Uieda, L., Scharroo, R., Wobbe, F., Smith, W.H.F., Tian, D.: The generic mapping tools version 6. Geochem. Geophys. Geosyst. **6**(11), 5556–5564 (2019)
40. Hutton, K., Woessner, J., Hauksson, E.: Earthquake monitoring in Southern California for seventy-seven years (1932–2008). Bull. Seismol. Soc. Am. **100**(2), 423–446 (2010)
41. PCI-2—PCI-Based Two-Channel AE Board & System, by Physical Acoustics
42. Bender, B.: Maximum likelihood estimation of b values for magnitude grouped data. Bull. Seismol. Soc. Am. **73**(3), 831–851 (1983)
43. Pacheco, J.F.E., Scholz, C.H., Sykes, L.R.: Changes in frequency-size relationship from small to large earthquakes. Nature **355**, 71–73 (1992)
44. Yoder, M.R., Holliday, J.R., Turcotte, D.L., Rundle, J.B.: A geometric frequency-magnitude scaling transition: measuring $b = 1.5$ for large earthquakes. Tectonophysics **532–535**, 167–174 (2012)
45. Kamer, Y., Hiemer, S.: Data-driven spatial b value estimation with applications to California seismicity: to b or not to b. J. Geophys. Res.: Solid Earth **120**(7), 5191–5214 (2015)
46. Plenkers, K., Schorlemmer, D., Kwiatek, G., JAGUARS Research Group: On the probability of detecting picoseismicity. Bull. Seismol. Soc. Am. **101**(6), 2579–2591, 12 (2011)

47. Kwiatek, G., Plenkers, K., Nakatani, M., Yabe, Y., Dresen, G., JAGUARS-Group: Frequency-magnitude characteristics down to magnitude −4.4 for induced seismicity recorded at Mponeng gold mine. Bull. Seismol. Soc. Am. **100**(3), 1165–1173, 06 (2010)
48. Kagan, Y.: Universality of the seismic moment-frequency relation. Pure Appl. Geophys. **155**, 537–573 (1999)